The phase of sensorimotor mu and beta oscillations has the opposite effect on corticospinal excitability

Miles Wischnewski[1], Zachary J. Haigh[1], Sina Shirinpour[1], Ivan Alekseichuk[1], Alexander Opitz[1]

[1]Department of Biomedical Engineering, University of Minnesota, Minneapolis, MN, United States of America

Corresponding authors:

Alexander Opitz, PhD
University of Minnesota
Department of Biomedical Engineering
E-mail: aopitz@umn.edu

Miles Wischnewski, PhD
University of Minnesota
Department of Biomedical Engineering
E-mail: mwischne@umn.edu

Total number of words: 4147

Figures: 5

Supplementary materials: yes

Keywords

Transcranial magnetic stimulation; Electroencephalography; Neural oscillation phase; Real-time neuromodulation; Mu oscillations; Beta oscillations; Primary motor cortex

Abstract

Background: Neural oscillations in the primary motor cortex (M1) shape corticospinal excitability. Power and phase of ongoing mu (8-13 Hz) and beta (14-30 Hz) activity may mediate motor cortical output. However, the functional dynamics of both mu and beta phase and power relationships and their interaction, are largely unknown.

Objective: Here, we employ recently developed real-time targeting of the mu and beta rhythm, to apply phase-specific brain stimulation and probe motor corticospinal excitability non-invasively. For this, we used instantaneous read-out and analysis of ongoing oscillations, targeting four different phases (0°, 90°, 180°, and 270°) of mu and beta rhythms with suprathreshold single-pulse transcranial magnetic stimulation (TMS) to M1. Ensuing motor evoked potentials (MEPs) in the right first dorsal interossei muscle were recorded. Twenty healthy adults took part in this double-blind randomized crossover study.

Results: Mixed model regression analyses showed significant phase-dependent modulation of corticospinal output by both mu and beta rhythm. Strikingly, these modulations exhibit a double dissociation. MEPs are larger at the mu trough and rising phase and smaller at the peak and falling phase. For the beta rhythm we found the opposite behavior. Also, mu power, but not beta power, was positively correlated with corticospinal output. Power and phase effects did not interact for either rhythm, suggesting independence between these aspects of oscillations.

Conclusion: Our results provide insights into real-time motor cortical oscillation dynamics, which offers the opportunity to improve the effectiveness of TMS by specifically targeting different frequency bands.

Introduction

Neocortical activity in the motor cortex is characterized by neural oscillations, foremost in the mu (8-13 Hz) and beta (14-30 Hz) rhythms. On the one hand, changes in their power correlate with motor functions such as preparation and execution of voluntary movement [1–7]. On the other hand, motor cortical output correlates with the phase of mu and beta oscillations [8–13]. This phase-dependency may result from synchronization of neural spiking activity and is thus phase-specifically coupled to the oscillatory envelope [14–18].

Although the coupling between cortical oscillation phase and spiking activity is well-established. However, the relationship between functional cortical excitability and phase of mu and particularly beta oscillations in the motor cortex remains to be fully understood. To provide causal evidence for a relation between oscillatory phase and cortical excitability, one needs to synchronize the electrocortical read-outs and causal probing of excitability with millisecond precision. Recent advances in real-time tracking of cortical oscillations and non-invasive modulation of motor cortex activity in healthy human participants have provided new insights [19–29]. Such real-time systems, combining electroencephalography (EEG) and transcranial magnetic stimulation (TMS), have provided evidence for a modulation of corticospinal excitability by motor cortical oscillatory phase and power [19,20,24,27].

Reports in non-human primates and patients with neurosurgical implants suggest that motor functioning is phase-dependent on oscillations in the motor cortical mu rhythm [13,15] Based on this, first pursuits on real-time detection of motor oscillation phase relationships in healthy volunteers have focused on the mu rhythm [19,20,22,23,27], Various studies suggest that motor evoked potential (MEP) amplitude is larger at the trough of the mu rhythm and smaller at the peak [19,22,23,27,30]. However, others have provided evidence that ongoing mu phase does

not significantly predict corticospinal excitation [20,24]. Rather, pre-stimulation mu power is suggested to determine MEP amplitude [19,20,24,31].

Whereas findings on associations between corticospinal excitability and mu phase are mixed, to the best of our knowledge, no result on real-time non-invasive neuromodulation of the beta rhythm has been published. Despite superficial similarities between mu and beta oscillations they reflect distinct functional sensorimotor networks and may have different anatomical origins [32–37]. As such, it is likely that phase-modulation of cortical excitability would reflect distinct patterns for mu and beta rhythms. Human and non-human primate studies have suggested a potential coupling of motor responses and motor cortical beta-phase [10,18,38,39]. Electrocorticography (ECoG) has shown phase-dependency of motor network beta-rhythm activity in Parkinson's disease patients [10,11,40,41]. Furthermore, beta phase-dependent stimulation in these patients has been shown to ameliorate motor deficits [42–44].

The absence of real-time TMS-EEG studies on beta rhythm may stem from the intrinsically lower signal-to-noise ratio, faster pace, and broader frequency band compared to mu oscillations. Additionally, it has been proposed that motor cortical beta oscillations partially reflect a harmonic of the mu rhythm (mu-beta), as it follows an arch-shape, rather than being sinusoidal [45,46]. To reliably target the beta phase in real-time, we optimized a cutting-edge real-time algorithm - Educated Temporal Prediction (ETP) - to perform accurate forward predictions during real-time phase targeting [25]. Due to its robustness to noise and fast processing time, ETP can accurately track and stimulate both mu and beta oscillations. Using our approach, we targeted mu and beta phase in the motor cortex in real-time. Our results show a double dissociation in the relationship between mu and beta phase on corticospinal excitability. That is, phases of mu oscillation that resulted in larger than average motor cortex output generate

smaller than average motor cortex output for the same phases of beta, and vice versa. Our data provide the first evidence for distinct phase-dependency of mu- and beta-mediated functional sensorimotor networks that modulate corticospinal excitability. Optimizing TMS-targeting to mu or beta phase can increase robustness of TMS with clear implications for improving the efficacy of TMS in clinical use.

Methods

Participants

We recruited 20 healthy volunteers (11 female, mean ± std age: 22.7 y ± 2.9) in this double-blinded randomized crossover study. Each participant visited for two sessions (targeting mu and beta oscillations). Participants were right-handed, between 18 and 45 years of age, without a history of neurological or psychiatric disorders, head injuries, or metal or electric implants in the head, neck, or chest area. Participants were not pre-selected on the basis of electrophysiological characteristics, such as motor threshold or sensorimotor oscillatory power. The study was approved by the institutional review board of the University of Minnesota and all volunteers gave written informed consent prior to participation.

Transcranial magnetic stimulation

We applied single-pulse biphasic TMS using the Magstim Rapid^2 with a figure-of-eight shaped D70^2 coil (Magstim Inc., Plymouth, MN, USA). The coil was placed over the left motor cortex, corresponding to the hotspot of the right first dorsal interossei (FDI) muscle, and oriented approximately at a 45° angle relative to the midline. Electromyography (EMG) was used to record motor-evoked potentials (MEP) from the FDI using self-adhesive, disposable electrodes.

EMG sampling rate was set to 10 kHz using a BIOPAC ERS100C amplifier (BIOPAC systems, Inc., Goleta, CA, USA). Initially, the motor hotspot, i.e. the location and orientation that leads to the largest MEP, was determined. Hotspot coordinates were stored and coil location and orientation in reference to the hotspot were continuously tracked using a Brainsight neuronavigation system (Rogue Research Inc., Montreal, Canada). At the hotspot, the resting motor threshold (RMT) was determined using an adaptive threshold-hunting algorithm [47]. The test intensity during the experimental session was set to 120% of RMT.

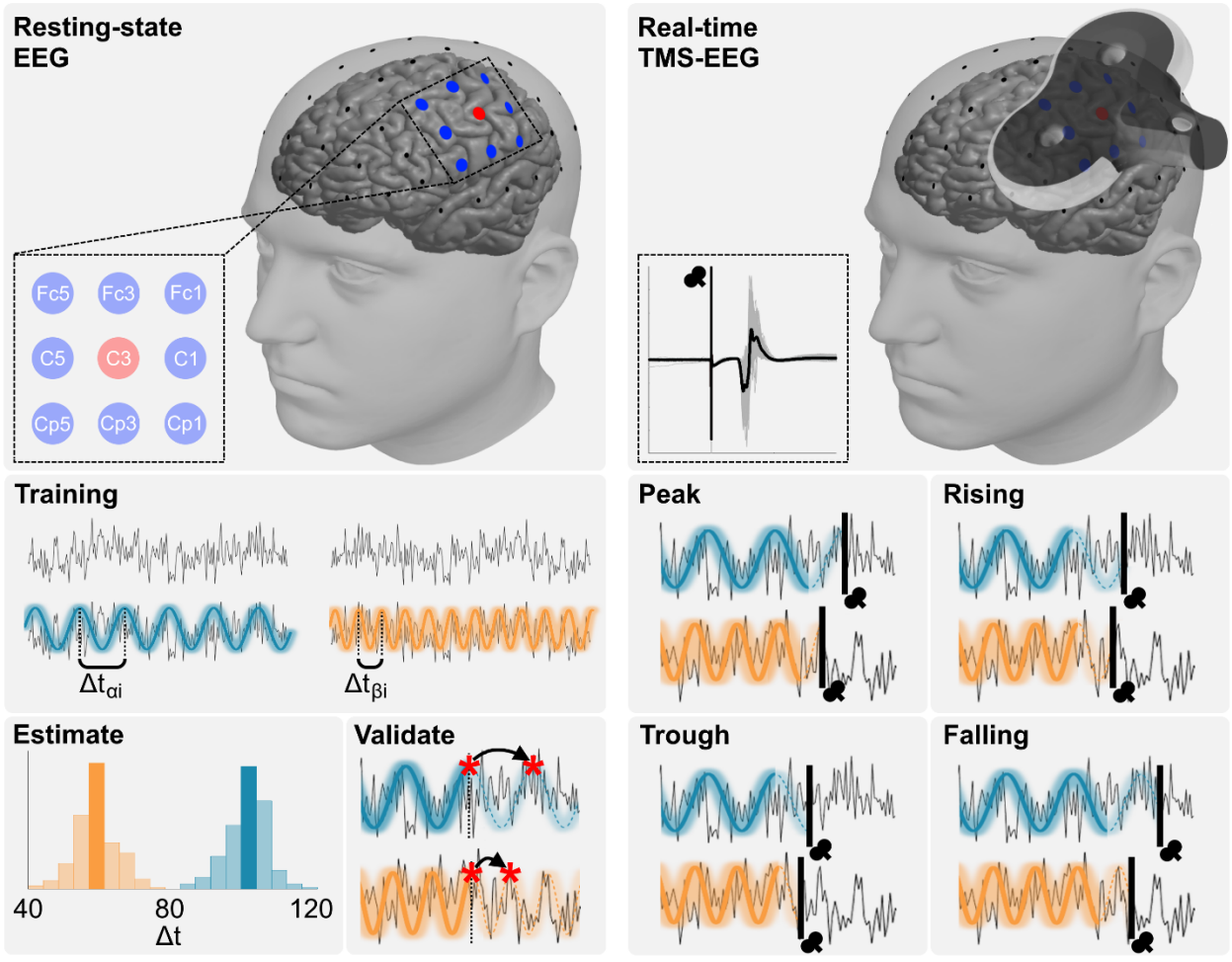

Figure 1. Overview of the educated temporal prediction (ETP) algorithm. Left: The algorithm is first trained using the resting state data from the sensorimotor cortex. Signals at sensorimotor cortex channel C3 are re-referenced using a center-surround Laplacian montage using 8 channels (Fc1, Fc3, Fc5, C1, C5, Cp1, Cp3, and Cp5). Depending on the experimental condition, we stimulated while tracking the phase of mu (8-13 Hz, blue) or beta (14-30 Hz, orange) range. From the resting-state data, the typical cycle length is extracted and used during the real-time stimulation. Right: During real-time application, EEG preprocessing follows the same pipeline as the training step. TMS is triggered at four different phases, namely peak (0°), rising phase (90°), trough (180°), or falling phase (270°). For each phase and oscillatory rhythm, we recorded MEPs from the FDI muscle.

EEG processing for real-time TMS triggering

Throughout the experiment, EEG was recorded using a 10-20 system, 64 active channel, TMS-compatible EEG system (actiCAP slim EEG cap, actiCHamp amplifier; Brain Products GmbH, Gilching, Germany). EEG data was streamed using Lab Streaming Layer (LSL) software to Matlab 2020b, where we used custom scripts to apply the ETP algorithm (Shirinpour et al., 2020). A sampling rate of 10 kHz with a 24-bits resolution per channel was used, and impedances were kept below 20 kΩ. Data was downsampled to 1 kHz. The electrode of interest for this experiment was C3, located over the hand knob of the left sensorimotor area. To extract mu and beta oscillations unique to the electrode of interest, a Laplacian reference method was used, where the mean of the 8 surrounding electrodes was subtracted from the signal measured at C3 (Figure 1). This Laplacian C3 signal was used for real-time stimulation, as well as for offline analysis of mu and beta power.

The EEG-TMS setup for real-time stimulation used here follows our previously validated implementation [25]. In short, the ETP algorithm uses resting-state data from a training step before the real-time application, which provides an initial estimate of individual temporal dynamics of cortical oscillations. For this, we record resting-state data for three minutes perform a C3 Laplacian spatial filtering, and clean the signal using a zero-phase FIR (Finite Impulse

Response) filter in the mu (8–13 Hz) or beta (14–30 Hz) range, as implemented in the Fieldtrip toolbox [48]. To obtain an undistorted ground truth, phase was based on the whole resting-state data (3 min). During the training, 500 ms sliding windows of the recorded data are used and signal edges after bandpass filtering (brick-wall filter) are removed. In doing so, we avoid ripples that can distort the data during filtering. Then, the algorithm estimates the typical cycle length (peak to peak interval) and validates its accuracy by simulating the accuracy of peak projection using the training data (Figure 1).

During real-time estimation, the calculated cycle length is adjusted to inform the forecasting algorithm that predicts upcoming peak, falling phase, trough, or rising phase (throughout this paper phase angles will be expressed in relation to a cosine, e.g. 0° is peak) of oscillation of interest and triggers TMS at the correct time. The EEG preprocessing pipeline during real-time measurements was the same as during the validation phase. Accuracy of ETP in targeting peak, falling, trough and rising phases for mu and beta is shown in Supplementary Figure 1. Overall processing delay of our system, i.e. the time between sending trigger and actual pulse delivery was accounted for in our algorithm to accurately deliver the TMS at the desired phases [25]. Real-time TMS-EEG was performed in four blocks of 150 pulses. Within each block, phases were applied pseudorandomly. The experimenter and the participant were blinded to the phase order. A jittered interval between 2 and 3 seconds between consecutive triggers was introduced to minimize the direct effects of previous trials. After this interval our algorithm targets the subsequent phase. Time between pulses was generally below 5 seconds (Supplementary Figure 2). Mu and beta oscillations were targeted in two different sessions, which were separated by at least 48 hours. The order of sessions was randomized. The sessions were performed at the same time of the day.

Data processing and analysis

MEP analysis

We calculated peak-to-peak MEP amplitude using a custom Matlab script. MEPs were identified in a window between 20 and 60 ms after the TMS pulse. Noise in the pre-TMS EMG can influence MEP amplitude and thus we excluded MEPs if average absolute EMG activity in a window from -100 to 0 ms before the TMS pulse was above 0.02 mV and larger than absolute average EMG activity + 2.5 times standard deviation of the resting state. For this resting state we used awindow of -500 to -400 ms before the TMS pulse and at least 1500 ms after the previous pulse, which is most likely captures a state of rest with no effects of the previous pulse [49]. All MEPs were visually inspected. Altogether, 3.3% of trials were removed (3.5% for targeting mu phases and 3.0% for targeting beta phases). For analysis, a participant's individual MEPs were normalized to the overall average of that participant. .

Offline EEG analysis

Pre-TMS power was analyzed offline for inclusion in the main analysis. Raw EEG data were re-referenced to the Laplacian C3 montage as was used for online analyses (Figure 1). Data were epoched in a window between -1000 and 0 milliseconds with respect to TMS trigger and a bandpass filter (2-50 Hz) was applied. Pre-TMS power was calculated by applying a fast Fourier transform with Hanning taper at a resolution of 1 Hz Furthermore, periodic and aperiodic signals were separated by using an Irregular Resampling Auto-Spectral Analysis (IRASA) [50] as implemented in FieldTrip [48]. Subsequently, we averaged power values between 8 and 13 Hz

(mu power, periodic), 14 and 30 Hz (beta power, periodic), and broadband aperiodic signals (2-50 Hz) at the single-trial level.

To investigate potential differences in mu and beta oscillation topography, sensor-level distributions were examined. Resting-state EEG data were re-referenced to a common average and filtered in the mu (8-13 Hz) and beta (14-30 Hz) bands, respectively. We estimated the pairwise correlations between the electrode of interest C3 to all other electrodes. Topographic plots were used to depict the spatial distribution of the correlations for mu and beta separately, as well as the difference between both conditions.

Since the mu-rhythm has been shown to follow an arch shape rather than a sinusoidal shape, power in the beta range may partially reflect harmonic activity of the mu rhythm [45,46]. Importantly, a priori our real-time algorithm is agnostic to whether activity in the beta frequency range results from a mu harmonic or from independent beta oscillations. To test for harmonicity, we calculated the ratio between the periods of bandpassed mu and beta oscillations.

Statistical analysis

In a trial level analysis, a general linear mixed-effects model (GLMM) was used on trial data with target phase (peak, falling, trough, rising) and target rhythm (mu, beta) as fixed effects variable and participant number as random effects variable. MEP amplitude was the dependent variable. Independently, after averaging MEPs per phase for each participant, Rayleigh's z-test of non-uniformity was performed for phase modulation at mu and beta oscillations.

As a follow up, to test the effects of pre-TMS power, two additional GLMMs were run on mu and beta conditions separately with pre-TMS power and phase as fixed effects variables. These analyses were followed up by post hoc subject-level simple linear regression models.

Additionally, we performed a group-level repeated-measures ANOVA on phase and target rhythm, followed by paired-samples t-tests. Subsequently, Spearman rank correlation between pre-TMS power and MEP amplitude for each subject and session were calculated.

Finally, a linear correlation was performed on the topographic distribution of mu and beta oscillations. This was followed by one-sample t-tests (test value = 0) on the Fisher z-transformed correlation data to test if the average deviates significantly from zero. For all analyses, significance level was set at $\alpha = 0.05$.

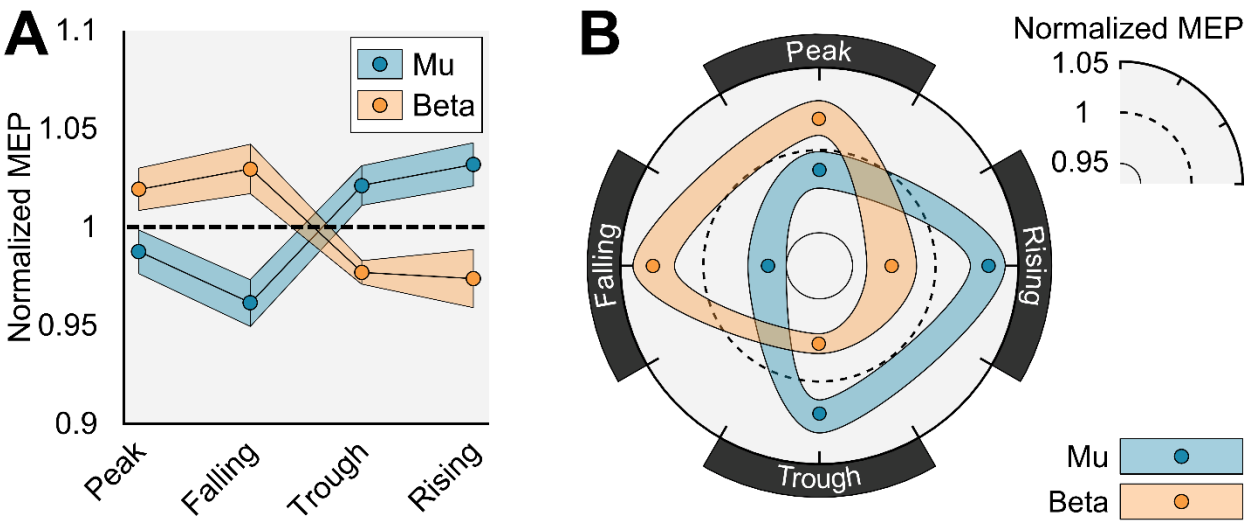

Figure 2. A) Group average (n = 20) ± standard error of mean of normalized MEPs for targeted phases in the mu and beta frequency. B) Circular representation of the data with smooth interpolation between conditions.

Results

Real-time TMS of ongoing cortical oscillations resulted in a double dissociation of phase relationships for mu and beta oscillations (Figure 2A). Accordingly, GLMM regression showed a significant interaction between target phase and target rhythm on MEP amplitude ($F = 16.42$, $p < 0.001$). Distinct phase relation patterns were confirmed by Rayleigh's test for non-uniformity of circular group level data. Normalized MEP amplitudes at phases of the mu rhythm were non-

uniformly distributed ($Z = 3.02$, $p = 0.048$), with a mean direction of the circular distribution of $\theta = 225.00°$ and circular dispersion of $\kappa = 29.27°$. Thus, MEP amplitudes were maximal when mu oscillations are at trough and rising phase (Figure 2B) and lower than average at the opposing phases. Normalized MEP amplitudes at phases of the beta rhythm were also non-uniformly distributed ($Z = 3.27$, $p = 0.037$), with circular mean of $\theta = 29.05°$ and dispersion of $\kappa = 30.53°$. This means that MEP amplitudes were maximal when beta oscillations are at peak or falling phase (Figure 2B) and again lower than average at the opposing phases.

The results of phase on MEPs were confirmed on the group level. A repeated-measures ANOVA showed a significant phase*target rhythm interaction ($F = 11.24$, $p < 0.001$), with no main effects for phase ($F = 0.16$, $p = 0.923$), or target rhythm ($F = 0.62$, $p = 0.440$). Post hoc t-tests showed differences between mu and beta peak falling phase ($t = 3.96$, $p < 0.001$), trough ($t = 4.37$, $p < 0.001$), and rising phase ($t = 3.10$, $p = 0.006$). The difference between mu and beta peak showed a non-significant trend ($t = 2.09$, $p = 0.051$).

The results are largely consistent at the individual level. The observed pattern of larger MEP amplitudes at the beta peak compared to the mu peak were observed in 13 out of 20 participants. Larger MEP amplitudes at beta falling compared to mu falling were observed in 14 out of 20 participants. Larger MEP amplitudes at mu trough compared to beta trough were observed in 18 out of 20 participants. Larger MEP amplitudes at mu rising compared to beta rising were observed in 14 out of 20 participants (Figure 3). Phase responses for both mu and beta per participant are shown in Supplementary Figure 3.

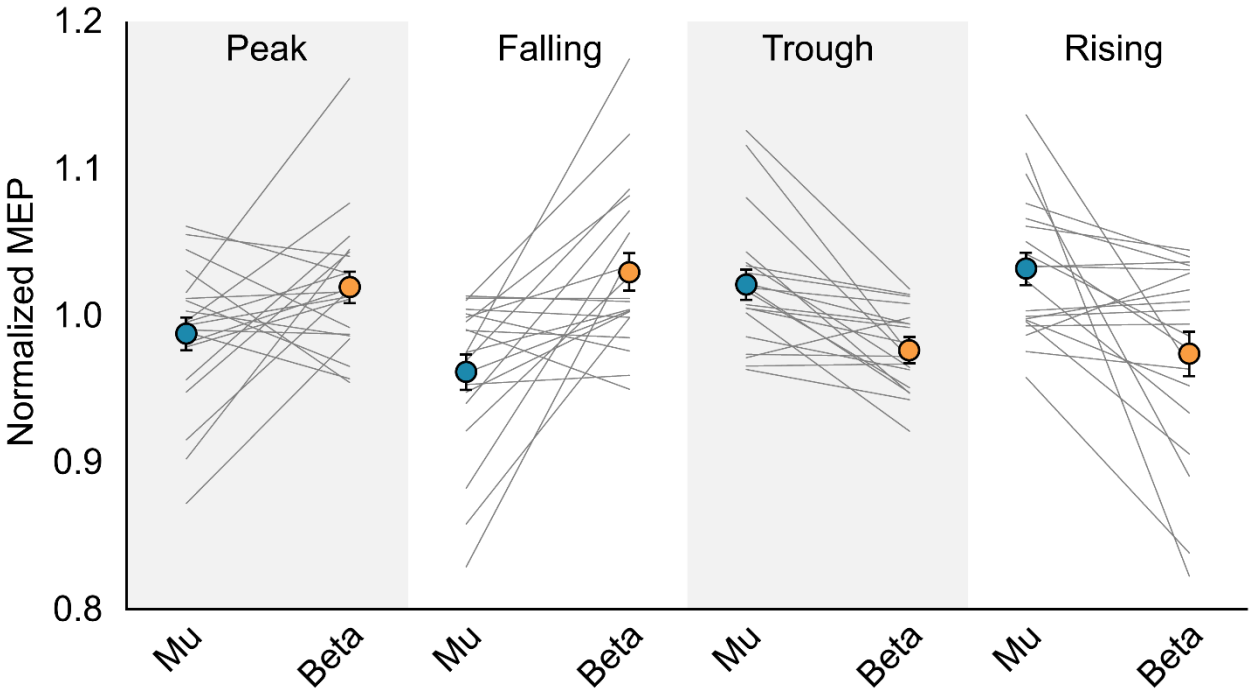

Figure 3. Individual phase-dependent modulation of MEP amplitude for mu and beta oscillations. Error bars represent standard error of mean.

In analyses of each target rhythm condition separately, we added pre-TMS power of the targeted rhythm and the aperiodic component. MEP amplitude during targeting of the mu rhythm was affected by both target phase ($F = 3.75$, $p = 0.011$) and pre-TMS periodic mu power ($F = 15.30$, $p < 0.001$). Crucially, however, no significant phase*power interaction was observed ($F = 1.77$, $p = 0.151$), suggesting that both power and phase affect MEP amplitude independently. At an individual level, correlation between mu power and MEP amplitude ranged between $\rho = -0.102$ and $\rho = 0.250$ (median $\rho = 0.055$). A one-sample t-test on the Fisher z-transformed correlation values confirmed that on average pre-TMS mu power shows a significant positive relationship with MEP amplitude ($t = 4.74$, $p < 0.001$). A significant positive relationship was observed in 15 out of 40 sessions, whereas a significant negative relationship was observed in 1 session (Figure 4A). MEP amplitude while targeting beta rhythm was affected by target phase

alone (F = 4.26, p = 0.005). No effect of pre-TMS periodic beta power (F = 0.24, p = 0.622), nor a phase*power interaction (F = 2.50, p = 0.058) was observed on MEP amplitude. At an individual level, correlation between beta power and MEP amplitude ranged between ρ = -0.168 and ρ = 0.151 (median ρ = -0.008). A one-sample t-test on the Fisher z-transformed correlation values confirmed that on average pre-TMS beta power does not significantly relate to MEP amplitude (t = 0.90, p = 0.375). A significant positive relationship was observed in 12 out of 40 sessions, whereas a significant negative relationship was observed in 4 out of 40 sessions (Figure 4B). Finally, MEP amplitude was not significantly affected by the aperiodic component of the power signal (F = 0.05, p = 0.821), nor a phase*power interaction (F = 0.02, p = 0.996)

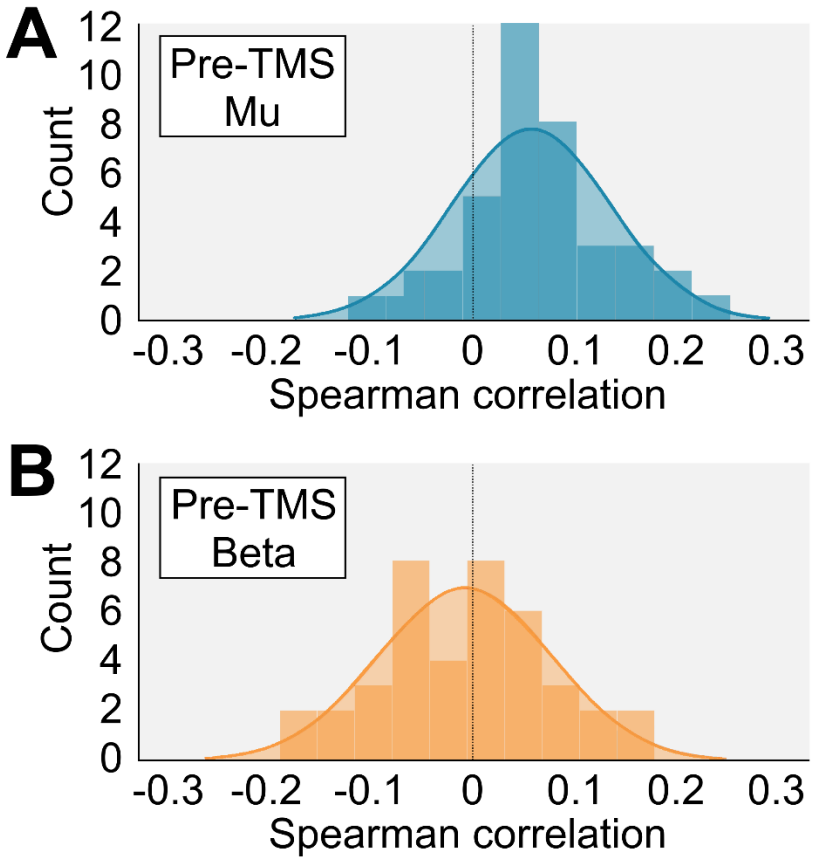

Figure 4. Histogram of individual Spearman correlations between MEP amplitude and A) pre-TMS mu power, and B) pre-TMS beta power after extracting the periodic components of each frequency band.

One possible confound could arise where channels in the Laplacian reference montage contribute differently to the target electrode between conditions. Therefore, we performed a sensor-level analysis of mu and beta distributions, by looking at the channel-to-channel correlations. Resulting topographic plots showed highly similar distributions for both mu and beta rhythms at sensor level (Figure 5). Distributions were highly correlated ($\rho = 0.92$, $p < 0.001$), suggesting that our main results cannot be explained by differences in mu and beta signal arrangement.

Finally, the typical arch-shape of the mu signal results in harmonics in the beta frequency range (referred to as mu-beta). To test whether our algorithm picked up a mu-harmonic or independent beta activity, we made a strict mathematical estimation of harmonicity between the signals and inspected individual power spectra (Supplementary Figure 4). By definition, the harmonic signals should have a period ratio that is an integer number. However, no integer values were observed with an average ratio of 2.148 and values for all participants and sessions ranging between 2.051 and 2.248. As such, we observed no indication for beta signals resulting from a mu harmonic. Furthermore, the phase relationship between mu and beta rhythms was generally weak, suggesting little dependence between phases of both signals (Supplementary Figure 5).

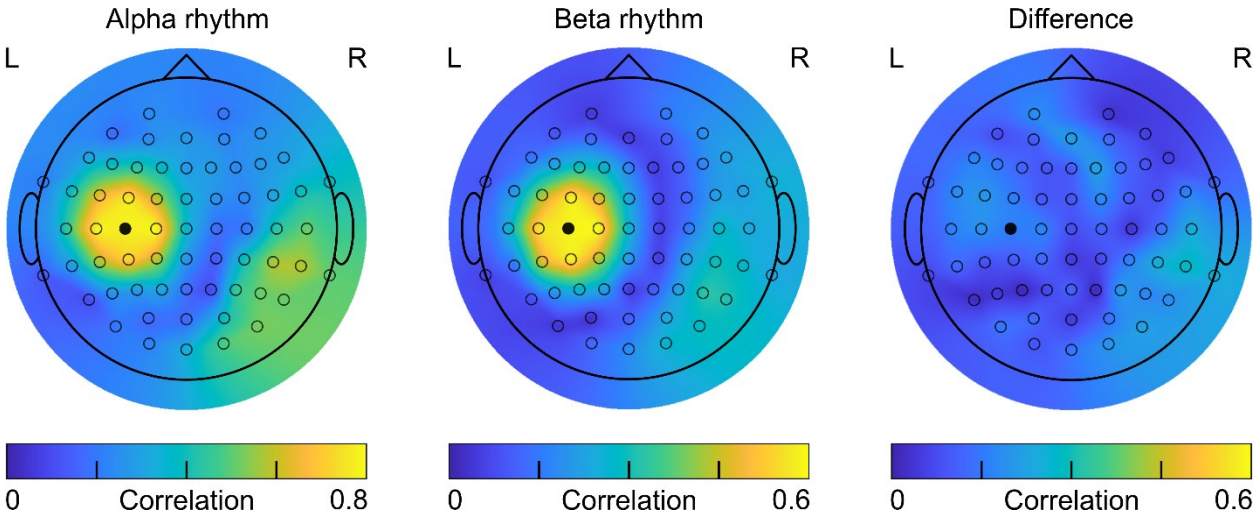

Figure 5. Spatial topographies for the recorded mu rhythm, beta rhythm, and the difference between both. Color map represents correlational values of electrode pairings between target electrode C3 and all other electrodes. The black electrode corresponds to C3.

Discussion

In this study, we demonstrate for the first time that mu and beta oscillation phase differentially modulate MEP amplitude. In summary, we found that I) phase of mu and beta oscillations picked up at sensorimotor channels modulate corticospinal excitation; II) this phase-dependent MEP modulation follows an opposing pattern for mu and beta; III) mu power, but not beta power, significantly modulates MEP amplitude; IV) modulation of MEP amplitudes by phase and power do not interact.

To our knowledge, we provide the first direct evidence for MEP amplitude modulation by beta phase, in addition to mu phase, measured with real-time TMS-EEG. Beta-phase dependency has been hinted at by previous offline TMS studies using post-hoc analyses [51–56]. Also, human subdural electrocorticographic (ECoG) recordings have shown that motor cortical beta activity is phase-locked to neural population activity during movement [10,41,43]. Furthermore, motor cortical spiking activity has been shown to be dependent on local field potential beta-

phase in non-human primates [38,57]. Sensorimotor beta oscillations have been suggested to arise from alternating de- and hyper-polarization of layer V pyramidal cells, mediated by phase-locked gamma-aminobutyric acid (GABA) mediated interneuron inputs [1,58–60]. Here we show that beta phase-dependency can be probed non-invasively in real-time. Our data showed largest MEP amplitudes during beta peak and falling phase (Figure 2). Salimpour et al. [44] applied real-time electrical motor cortex stimulation in Parkinson's disease patients during surgery. Although direct comparison of results from electrical stimulation and ECoG data to ours may be challenging, it is interesting to point out that phase-dependency was similar, with beta peak and falling phase leading to the largest motor output.

We found no dependency of beta power on MEP amplitude, nor was there an interaction between beta phase and power, in line with previous findings [51,54,61–63]. This should not imply that beta oscillations are not related to motor output and evidence from previous research suggests that the relationship between beta oscillations and motor activation is complex. Pre-movement reduction of beta power has been associated with faster voluntary movement [64]. Chronic elevation of beta power, observed in Parkinson's disease has been related to difficulty initiating and controlling movements [65–67]. Furthermore, in addition to low-amplitude ongoing beta activity, high-amplitude beta bursts are suggested to be positively correlated to movement control [11,38,68–70]. Although these behavioral studies imply that beta power and beta bursts are crucial for endogenous control of voluntary movement, our and previous studies suggest that they are not related to exogenously probed cortico-spinal excitability [51,62,63]. Furthermore, Peters and colleagues [63] found that pre-TMS resting beta power does not affect the propagation of TMS excitations throughout the cortical-subcortical motor network.

Therefore, it seems that beta power may be a predictor for corticospinal activation during voluntary or task-related motor control, but not during resting-state motor excitability per se.

Additionally, we found that corticospinal excitation was modulated by the mu rhythm with an opposite phase relationship compared to beta oscillations. Various studies previously indicated mu phase-dependent modulation of MEP amplitudes, with larger responses at the mu trough compared to mu peak [19,22,23,27,30]. Our results confirm these findings on mu peak and trough, but the phase effects extended towards the subsequent falling and rising phase respectively. That is, we show that trough and rising phase yield largest corticospinal excitation, whereas mu peak and falling yield the smallest motor cortex activation (Figure 2).

Pre-stimulus mu power was a significant predictor for corticospinal excitability, but did not interact with mu phase, suggesting independence between mu power and phase. Subject-level positive correlations were observed in majority of subjects. Although the observed relationship was relatively weak - correlations varying between -0.1 and 0.25 - it is in line with previous observations [19,24,31,54]. However, others have found no relationship between mu power and MEP amplitude [8,27], or even a negative association [20,71,72]. At a first glance, a positive relationship between mu power and corticospinal activity seems counterintuitive since sensorimotor mu oscillations are related to GABAa-mediated inhibitory activity [19]. Also, higher mu power has been shown to reduce TMS-induced blood oxygenation level-dependent (BOLD) responses throughout the cortical-subcortical motor network [63]. However, mu oscillations are thought to predominantly originate from the somatosensory cortex [32–37]. Interconnections between somatosensory and primary motor cortex comprise of an intricate network of excitatory and inhibitory reciprocal connections. Increased mu power may reflect feedforward inhibition to primary motor cortex resulting in local disinhibition, which could

362 explain a positive relationship between mu power and MEP amplitudes. Although our findings
363 do agree with previous reports [19,24,31,54]. One important aspect may be to extract the
364 periodic components of the power spectra [50,73], which may explain why this positive
365 relationship was not found by others.

366 Sensorimotor mu and beta oscillations have been suggested to stem from distinct neural
367 origins [32–37]. Specifically, mu oscillations are proposed to originate pre-dominantly from the
368 post-central gyrus [36,37], although pre-central origins of mu have been reported as well
369 [35,74,75]. In contrast, beta oscillations are thought to stem from pre-central primary motor
370 cortex [4,36,37,76], but are also observed in post-central somatosensory cortex [4,75,77].
371 Although our study cannot make inferences on the source of mu and beta oscillations, sensor-
372 level signal distributions were highly similar (Figure 5). Similar scalp-level topographies suggest
373 that potential differences in neural origin did not influence phase detection during real-time
374 stimulation. A potential explanation for the opposing phase-relationship we observed results
375 from differences in axonal orientation within mu and beta sources. This possibility could be
376 investigated in future studies.

377 The sensorimotor mu-signal tends to resemble an arch-shape, rather than a sinusoid
378 [36,45,46,78]. As a result of this higher-frequency harmonics can be observed in the frequency
379 spectra. Particularly first-order harmonics would appear in the beta frequency range (referred to
380 as mu-beta). It is worth nothing that our ETP algorithm used here is agnostic to the origin of beta
381 oscillations. However, the opposing results in MEP amplitudes between mu and beta phase
382 would be unexpected since mu harmonics reflect similar functional properties [78]. Additionally,
383 we formally tested for harmonicity and found no evidence for it (Supplementary Figure 4 and 5).
384 Thus, we believe that the modulation of MEPs when targeting at frequencies between 14 and 30

Hz results from independent beta oscillations. A further limitation of this study is that phase accuracy was only established in the beginning of a session. Although we previously have shown that phase targeting with ETP is stable on average of a single session [25], individual fluctuations in oscillatory activity over time may affect targeting accuracy.

Our findings are crucial for the improvement of TMS effectiveness for treatment of neurological and psychiatric disorders. Targeting optimal rhythms with repetitive TMS could decrease variability of TMS outcomes [27,79]. For instance, targeting optimal oscillation phase could improve efficacy of TMS in the recovery of stroke [80] and treatment of major depressive disorder [28]. In this study, to our knowledge, we were able to non-invasively target the beta rhythm in real-time reliably for the first time. In future work it will be crucial to further optimize real-time and closed-loop systems, in order to target different oscillatory rhythms, and different spatial locations [81–83]. Eventually, this will allow for adaptive non-invasive neuromodulation that can provide personalized decoding of on-going brain states. This individualization can greatly benefit clinical application of TMS, by reducing variability between and within patients.

Conflict of interest

Authors declare no conflict of interest.

References

[1] Baker SN. Oscillatory interactions between sensorimotor cortex and the periphery. Curr Opin Neurobiol 2007;17:649–55. https://doi.org/10.1016/j.conb.2008.01.007.

[2] Baker SN, Pinches EM, Lemon RN. Synchronization in monkey motor cortex during a precision grip task. II. effect of oscillatory activity on corticospinal output. J Neurophysiol 2003;89:1941–53. https://doi.org/10.1152/jn.00832.2002.

[3] Jenkinson N, Brown P. New insights into the relationship between dopamine, beta oscillations and motor function. Trends Neurosci 2011;34:611–8. https://doi.org/10.1016/j.tins.2011.09.003.

[4] Jurkiewicz MT, Gaetz WC, Bostan AC, Cheyne D. Post-movement beta rebound is generated in motor cortex: Evidence from neuromagnetic recordings. NeuroImage 2006;32:1281–9. https://doi.org/10.1016/j.neuroimage.2006.06.005.

[5] Pfurtscheller G, Stancák A, Neuper C. Post-movement beta synchronization. A correlate of an idling motor area? Electroencephalogr Clin Neurophysiol 1996;98:281–93. https://doi.org/10.1016/0013-4694(95)00258-8.

[6] Pfurtscheller G, Lopes da Silva FH. Event-related EEG/MEG synchronization and desynchronization: basic principles. Clin Neurophysiol 1999;110:1842–57. https://doi.org/10.1016/S1388-2457(99)00141-8.

[7] Saleh M, Reimer J, Penn R, Ojakangas CL, Hatsopoulos NG. Fast and slow oscillations in human primary motor cortex predict oncoming behaviorally relevant cues. Neuron 2010;65:461–71. https://doi.org/10.1016/j.neuron.2010.02.001.

[8] Berger B, Minarik T, Liuzzi G, Hummel FC, Sauseng P. EEG oscillatory phase-dependent markers of corticospinal excitability in the resting brain. BioMed Res Int 2014;2014:e936096. https://doi.org/10.1155/2014/936096.

[9] Combrisson E, Perrone-Bertolotti M, Soto JL, Alamian G, Kahane P, Lachaux J-P, et al. From intentions to actions: Neural oscillations encode motor processes through phase,

amplitude and phase-amplitude coupling. NeuroImage 2017;147:473–87. https://doi.org/10.1016/j.neuroimage.2016.11.042.

[10] Miller KJ, Hermes D, Honey CJ, Hebb AO, Ramsey NF, Knight RT, et al. Human motor cortical activity is selectively phase-entrained on underlying rhythms. PLoS Comput Biol 2012;8:e1002655. https://doi.org/10.1371/journal.pcbi.1002655.

[11] O'Keeffe AB, Malekmohammadi M, Sparks H, Pouratian N. Synchrony drives motor cortex beta bursting, waveform dynamics, and phase-amplitude coupling in Parkinson's disease. J Neurosci 2020;40:5833–46. https://doi.org/10.1523/JNEUROSCI.1996-19.2020.

[12] Takahashi K, Kim S, Coleman TP, Brown KA, Suminski AJ, Best MD, et al. Large-scale spatiotemporal spike patterning consistent with wave propagation in motor cortex. Nat Commun 2015;6:7169. https://doi.org/10.1038/ncomms8169.

[13] Yanagisawa T, Yamashita O, Hirata M, Kishima H, Saitoh Y, Goto T, et al. Regulation of motor representation by phase–amplitude coupling in the sensorimotor cortex. J Neurosci 2012;32:15467–75. https://doi.org/10.1523/JNEUROSCI.2929-12.2012.

[14] Fetz EE, Chen D, Murthy VN, Matsumura M. Synaptic interactions mediating synchrony and oscillations in primate sensorimotor cortex. J Physiol-Paris 2000;94:323–31. https://doi.org/10.1016/S0928-4257(00)01089-5.

[15] Haegens S, Nácher V, Luna R, Romo R, Jensen O. α-Oscillations in the monkey sensorimotor network influence discrimination performance by rhythmical inhibition of neuronal spiking. Proc Natl Acad Sci 2011;108:19377–82. https://doi.org/10.1073/pnas.1117190108.

[16] Johnson L, Alekseichuk I, Krieg J, Doyle A, Yu Y, Vitek J, et al. Dose-dependent effects of transcranial alternating current stimulation on spike timing in awake nonhuman primates. Sci Adv 2020:9.

[17] Murthy VN, Fetz EE. Coherent 25- to 35-Hz oscillations in the sensorimotor cortex of awake behaving monkeys. Proc Natl Acad Sci 1992;89:5670–4. https://doi.org/10.1073/pnas.89.12.5670.

[18] Murthy VN, Fetz EE. Synchronization of neurons during local field potential oscillations in sensorimotor cortex of awake monkeys. J Neurophysiol 1996;76:3968–82. https://doi.org/10.1152/jn.1996.76.6.3968.

[19] Bergmann TO, Lieb A, Zrenner C, Ziemann U. Pulsed facilitation of corticospinal excitability by the sensorimotor μ-alpha rhythm. J Neurosci 2019;39:10034–43. https://doi.org/10.1523/JNEUROSCI.1730-19.2019.

[20] Madsen KH, Karabanov AN, Krohne LG, Safeldt MG, Tomasevic L, Siebner HR. No trace of phase: Corticomotor excitability is not tuned by phase of pericentral mu-rhythm. Brain Stimulat 2019;12:1261–70. https://doi.org/10.1016/j.brs.2019.05.005.

[21] Sasaki K, Fujishige Y, Kikuchi Y, Odagaki M. A transcranial magnetic stimulation trigger system for suppressing motor-evoked potential fluctuation using electroencephalogram coherence analysis: algorithm development and validation study. JMIR Biomed Eng 2021;6:e28902. https://doi.org/10.2196/28902.

[22] Schaworonkow N, Caldana Gordon P, Belardinelli P, Ziemann U, Bergmann TO, Zrenner C. M-rhythm extracted with personalized EEG filters correlates with corticospinal excitability in real-time phase-triggered EEG-TMS. Front Neurosci 2018;12.

[23] Schaworonkow N, Triesch J, Ziemann U, Zrenner C. EEG-triggered TMS reveals stronger brain state-dependent modulation of motor evoked potentials at weaker stimulation intensities. Brain Stimulat 2019;12:110–8. https://doi.org/10.1016/j.brs.2018.09.009.

[24] Karabanov AN, Madsen KH, Krohne LG, Siebner HR. Does pericentral mu-rhythm "power" corticomotor excitability? – A matter of EEG perspective. Brain Stimulat 2021;14:713–22. https://doi.org/10.1016/j.brs.2021.03.017.

[25] Shirinpour S, Alekseichuk I, Mantell K, Opitz A. Experimental evaluation of methods for real-time EEG phase-specific transcranial magnetic stimulation. J Neural Eng 2020;17:046002. https://doi.org/10.1088/1741-2552/ab9dba.

[26] Zrenner C, Belardinelli P, Müller-Dahlhaus F, Ziemann U. Closed-loop neuroscience and non-invasive brain stimulation: a tale of two loops. Front Cell Neurosci 2016;10.

[27] Zrenner C, Desideri D, Belardinelli P, Ziemann U. Real-time EEG-defined excitability states determine efficacy of TMS-induced plasticity in human motor cortex. Brain Stimulat 2018;11:374–89. https://doi.org/10.1016/j.brs.2017.11.016.

[28] Zrenner B, Zrenner C, Gordon PC, Belardinelli P, McDermott EJ, Soekadar SR, et al. Brain oscillation-synchronized stimulation of the left dorsolateral prefrontal cortex in depression using real-time EEG-triggered TMS. Brain Stimulat 2020;13:197–205. https://doi.org/10.1016/j.brs.2019.10.007.

[29] Hussain SJ, Vollmer MK, Stimely J, Norato G, Zrenner C, Ziemann U, et al. Phase-dependent offline enhancement of human motor memory. Brain Stimulat 2021;14:873–83. https://doi.org/10.1016/j.brs.2021.05.009.

[30] Desideri D, Zrenner C, Ziemann U, Belardinelli P. Phase of sensorimotor μ-oscillation modulates cortical responses to transcranial magnetic stimulation of the human motor cortex. J Physiol 2019;597:5671–86. https://doi.org/10.1113/JP278638.

[31] Thies M, Zrenner C, Ziemann U, Bergmann TO. Sensorimotor mu-alpha power is positively related to corticospinal excitability. Brain Stimulat 2018;11:1119–22. https://doi.org/10.1016/j.brs.2018.06.006.

[32] Gaetz W, Cheyne D. Localization of sensorimotor cortical rhythms induced by tactile stimulation using spatially filtered MEG. NeuroImage 2006;30:899–908. https://doi.org/10.1016/j.neuroimage.2005.10.009.

[33] Jones SR, Pritchett DL, Sikora MA, Stufflebeam SM, Hämäläinen M, Moore CI. Quantitative analysis and biophysically realistic neural modeling of the MEG mu rhythm: Rhythmogenesis and modulation of sensory-evoked responses. J Neurophysiol 2009;102:3554–72. https://doi.org/10.1152/jn.00535.2009.

[34] Premoli I, Bergmann TO, Fecchio M, Rosanova M, Biondi A, Belardinelli P, et al. The impact of GABAergic drugs on TMS-induced brain oscillations in human motor cortex. NeuroImage 2017;163:1–12. https://doi.org/10.1016/j.neuroimage.2017.09.023.

[35] Ronnqvist K, McAllister C, Woodhall G, Stanford I, Hall S. A multimodal perspective on the composition of cortical oscillations. Front Hum Neurosci 2013;7.

[36] Salmelin R, Hari R. Spatiotemporal characteristics of sensorimotor neuromagnetic rhythms related to thumb movement. Neuroscience 1994;60:537–50. https://doi.org/10.1016/0306-4522(94)90263-1.

[37] Salmelin R, Hámáaláinen M, Kajola M, Hari R. Functional segregation of movement-related rhythmic activity in the human brain. NeuroImage 1995;2:237–43. https://doi.org/10.1006/nimg.1995.1031.

[38] Reimer J, Hatsopoulos NG. Periodicity and evoked responses in motor cortex. J Neurosci 2010;30:11506–15. https://doi.org/10.1523/JNEUROSCI.5947-09.2010.

[39] Peles O, Werner-Reiss U, Bergman H, Israel Z, Vaadia E. Phase-specific microstimulation differentially modulates beta oscillations and affects behavior. Cell Rep 2020;30:2555-2566.e3. https://doi.org/10.1016/j.celrep.2020.02.005.

[40] Bouthour W, Mégevand P, Donoghue J, Lüscher C, Birbaumer N, Krack P. Biomarkers for closed-loop deep brain stimulation in Parkinson disease and beyond. Nat Rev Neurol 2019;15:343–52. https://doi.org/10.1038/s41582-019-0166-4.

[41] de Hemptinne C, Ryapolova-Webb ES, Air EL, Garcia PA, Miller KJ, Ojemann JG, et al. Exaggerated phase–amplitude coupling in the primary motor cortex in Parkinson disease. Proc Natl Acad Sci 2013;110:4780–5. https://doi.org/10.1073/pnas.1214546110.

[42] Cagnan H, Pedrosa D, Little S, Pogosyan A, Cheeran B, Aziz T, et al. Stimulating at the right time: phase-specific deep brain stimulation. Brain 2017;140:132–45. https://doi.org/10.1093/brain/aww286.

[43] Holt AB, Kormann E, Gulberti A, Pötter-Nerger M, McNamara CG, Cagnan H, et al. Phase-dependent suppression of beta oscillations in Parkinson's disease patients. J Neurosci 2019;39:1119–34. https://doi.org/10.1523/JNEUROSCI.1913-18.2018.

[44] Salimpour Y, Mills KA, Hwang BY, Anderson WS. Phase- targeted stimulation modulates phase-amplitude coupling in the motor cortex of the human brain. Brain Stimulat 2022;15:152–63. https://doi.org/10.1016/j.brs.2021.11.019.

[45] Cole SR, Voytek B. Brain oscillations and the importance of waveform shape. Trends Cogn Sci 2017;21:137–49. https://doi.org/10.1016/j.tics.2016.12.008.

[46] Triggiani AI, Valenzano A, Del Percio C, Marzano N, Soricelli A, Petito A, et al. Resting state Rolandic mu rhythms are related to activity of sympathetic component of autonomic nervous system in healthy humans. Int J Psychophysiol 2016;103:79–87. https://doi.org/10.1016/j.ijpsycho.2015.02.009.

[47] Julkunen P. Mobile application for adaptive threshold hunting in transcranial magnetic stimulation. IEEE Trans Neural Syst Rehabil Eng 2019;27:1504–10. https://doi.org/10.1109/TNSRE.2019.2925904.

[48] Oostenveld R, Fries P, Maris E, Schoffelen J-M. FieldTrip: open source software for advanced analysis of meg, eeg, and invasive electrophysiological data. Comput Intell Neurosci 2010;2011:e156869. https://doi.org/10.1155/2011/156869.

[49] Wischnewski M, Kowalski GM, Rink F, Belagaje SR, Haut MW, Hobbs G, et al. Demand on skillfulness modulates interhemispheric inhibition of motor cortices. J Neurophysiol 2016;115:2803–13. https://doi.org/10.1152/jn.01076.2015.

[50] Wen H, Liu Z. Separating fractal and oscillatory components in the power spectrum of neurophysiological signal. Brain Topogr 2016;29:13–26. https://doi.org/10.1007/s10548-015-0448-0.

[51] Hussain SJ, Claudino L, Bönstrup M, Norato G, Cruciani G, Thompson R, et al. Sensorimotor oscillatory phase–power interaction gates resting human corticospinal output. Cereb Cortex 2019;29:3766–77. https://doi.org/10.1093/cercor/bhy255.

[52] Keil J, Timm J, SanMiguel I, Schulz H, Obleser J, Schönwiesner M. Cortical brain states and corticospinal synchronization influence TMS-evoked motor potentials. J Neurophysiol 2014;111:513–9. https://doi.org/10.1152/jn.00387.2013.

[53] Khademi F, Royter V, Gharabaghi A. Distinct beta-band oscillatory circuits underlie corticospinal gain modulation. Cereb Cortex 2018;28:1502–15. https://doi.org/10.1093/cercor/bhy016.

[54] Schilberg L, Oever ST, Schuhmann T, Sack AT. Phase and power modulations on the amplitude of TMS-induced motor evoked potentials. PLOS ONE 2021;16:e0255815. https://doi.org/10.1371/journal.pone.0255815.

[55] Torrecillos F, Falato E, Pogosyan A, West T, Di Lazzaro V, Brown P. Motor cortex inputs at the optimum phase of beta cortical oscillations undergo more rapid and less variable corticospinal propagation. J Neurosci 2020;40:369–81. https://doi.org/10.1523/JNEUROSCI.1953-19.2019.

[56] Van Elswijk G, Maij F, Schoffelen J-M, Overeem S, Stegeman DF, Fries P. Corticospinal beta-band synchronization entails rhythmic gain modulation. J Neurosci 2010;30:4481–8. https://doi.org/10.1523/JNEUROSCI.2794-09.2010.

[57] Witham CL, Wang M, Baker SN. Cells in somatosensory areas show synchrony with beta oscillations in monkey motor cortex. Eur J Neurosci 2007;26:2677–86. https://doi.org/10.1111/j.1460-9568.2007.05890.x.

[58] Bhatt MB, Bowen S, Rossiter HE, Dupont-Hadwen J, Moran RJ, Friston KJ, et al. Computational modelling of movement-related beta-oscillatory dynamics in human motor cortex. NeuroImage 2016;133:224–32. https://doi.org/10.1016/j.neuroimage.2016.02.078.

[59] Rossiter HE, Davis EM, Clark EV, Boudrias M-H, Ward NS. Beta oscillations reflect changes in motor cortex inhibition in healthy ageing. NeuroImage 2014;91:360–5. https://doi.org/10.1016/j.neuroimage.2014.01.012.

[60] Lacey MG, Gooding-Williams G, Prokic EJ, Yamawaki N, Hall SD, Stanford IM, et al. Spike firing and IPSPs in layer v pyramidal neurons during beta oscillations in rat primary motor cortex (M1) in vitro. PLOS ONE 2014;9:e85109. https://doi.org/10.1371/journal.pone.0085109.

[61] Mitchell WK, Baker MR, Baker SN. Muscle responses to transcranial stimulation in man depend on background oscillatory activity. J Physiol 2007;583:567–79. https://doi.org/10.1113/jphysiol.2007.134031.

[62] Ogata K, Nakazono H, Uehara T, Tobimatsu S. Prestimulus cortical EEG oscillations can predict the excitability of the primary motor cortex. Brain Stimulat 2019;12:1508–16. https://doi.org/10.1016/j.brs.2019.06.013.

[63] Peters JC, Reithler J, Graaf TA de, Schuhmann T, Goebel R, Sack AT. Concurrent human TMS-EEG-fMRI enables monitoring of oscillatory brain state-dependent gating of cortico-subcortical network activity. Commun Biol 2020;3:1–11. https://doi.org/10.1038/s42003-020-0764-0.

[64] Khanna P, Carmena JM. Beta band oscillations in motor cortex reflect neural population signals that delay movement onset. ELife 2017;6:e24573. https://doi.org/10.7554/eLife.24573.

[65] Brown P. Bad oscillations in Parkinson's disease. In: Riederer P, Reichmann H, Youdim MBH, Gerlach M, editors. Park. Dis. Relat. Disord., Vienna: Springer; 2006, p. 27–30. https://doi.org/10.1007/978-3-211-45295-0_6.

[66] Cannon J, McCarthy MM, Lee S, Lee J, Börgers C, Whittington MA, et al. Neurosystems: brain rhythms and cognitive processing. Eur J Neurosci 2014;39:705–19. https://doi.org/10.1111/ejn.12453.

[67] Kühn AA, Kupsch A, Schneider G-H, Brown P. Reduction in subthalamic 8–35 Hz oscillatory activity correlates with clinical improvement in Parkinson's disease. Eur J Neurosci 2006;23:1956–60. https://doi.org/10.1111/j.1460-9568.2006.04717.x.

[68] Bonaiuto JJ, Little S, Neymotin SA, Jones SR, Barnes GR, Bestmann S. Laminar dynamics of high amplitude beta bursts in human motor cortex. NeuroImage 2021;242:118479. https://doi.org/10.1016/j.neuroimage.2021.118479.

[69] Chen D, Fetz EE. Characteristic membrane potential trajectories in primate sensorimotor cortex neurons recorded in vivo. J Neurophysiol 2005;94:2713–25. https://doi.org/10.1152/jn.00024.2005.

[70] Feingold J, Gibson DJ, DePasquale B, Graybiel AM. Bursts of beta oscillation differentiate postperformance activity in the striatum and motor cortex of monkeys performing movement tasks. Proc Natl Acad Sci 2015;112:13687–92. https://doi.org/10.1073/pnas.1517629112.

[71] Sauseng P, Klimesch W, Gerloff C, Hummel FC. Spontaneous locally restricted EEG alpha activity determines cortical excitability in the motor cortex. Neuropsychologia 2009;47:284–8. https://doi.org/10.1016/j.neuropsychologia.2008.07.021.

[72] Zarkowski P, Shin CJ, Dang T, Russo J, Avery D. EEG and the variance of motor evoked potential amplitude. Clin EEG Neurosci 2006;37:247–51. https://doi.org/10.1177/155005940603700316.

[73] Donoghue T, Haller M, Peterson EJ, Varma P, Sebastian P, Gao R, et al. Parameterizing neural power spectra into periodic and aperiodic components. Nat Neurosci 2020;23:1655–65. https://doi.org/10.1038/s41593-020-00744-x.

[74] Smit DJA, Linkenkaer-Hansen K, Geus EJC de. Long-range temporal correlations in resting-state alpha oscillations predict human timing-error dynamics. J Neurosci 2013;33:11212–20. https://doi.org/10.1523/JNEUROSCI.2816-12.2013.

[75] Szurhaj W, Derambure P, Labyt E, Cassim F, Bourriez J-L, Isnard J, et al. Basic mechanisms of central rhythms reactivity to preparation and execution of a voluntary movement: a stereoelectroencephalographic study. Clin Neurophysiol 2003;114:107–19. https://doi.org/10.1016/S1388-2457(02)00333-4.

[76] Donoghue JP, Sanes JN, Hatsopoulos NG, Gaál G. Neural discharge and local field potential oscillations in primate motor cortex during voluntary movements. J Neurophysiol 1998;79:159–73. https://doi.org/10.1152/jn.1998.79.1.159.

[77] Brovelli A, Ding M, Ledberg A, Chen Y, Nakamura R, Bressler SL. Beta oscillations in a large-scale sensorimotor cortical network: Directional influences revealed by Granger causality. Proc Natl Acad Sci 2004;101:9849–54. https://doi.org/10.1073/pnas.0308538101.

[78] Pfurtscheller G, Brunner C, Schlögl A, Lopes da Silva FH. Mu rhythm (de)synchronization and EEG single-trial classification of different motor imagery tasks. NeuroImage 2006;31:153–9. https://doi.org/10.1016/j.neuroimage.2005.12.003.

[79] Baur D, Galevska D, Hussain S, Cohen LG, Ziemann U, Zrenner C. Induction of LTD-like corticospinal plasticity by low-frequency rTMS depends on pre-stimulus phase of sensorimotor μ-rhythm. Brain Stimulat 2020;13:1580–7. https://doi.org/10.1016/j.brs.2020.09.005.

[80] Hussain SJ, Hayward W, Fourcand F, Zrenner C, Ziemann U, Buch ER, et al. Phase-dependent transcranial magnetic stimulation of the lesioned hemisphere is accurate after stroke. Brain Stimulat 2020;13:1354–7. https://doi.org/10.1016/j.brs.2020.07.005.

Funding

Research presented here was supported by the University of Minnesota's MnDRIVE Initiative NSF Career Grant 2143852.